The following supplement accompanies the article

Coral reef benthic regimes exhibit non-linear threshold responses to natural physical drivers

Jamison M. Gove*, Gareth J. Williams, Margaret A. McManus, Susan J. Clark, Julia S. Ehses, Lisa M. Wedding

*Corresponding author: jamison.gove@noaa.gov

Marine Ecology Progress Series 522: 33–48 (2015)

Supplemental methods

Geomorphological data: Multibeam bathymetric data were collected during NOAA's Reef Assessment and Monitoring Program (RAMP) surveys of Palmyra aboard the NOAA Ship *Hi'ialakai* and the survey launch R/V *AHI* (Acoustic Habitat Investigator). The *Hi'ialakai* is equipped with two Kongsberg/Simrad multibeam sonars: a 30 kHz EM300 with mapping capability from ~100 to 3000+ m and a 300 kHz EM3002D with mapping capability from ~5 to 150 m. The R/V AHI has a 240 kHz Reson 8101ER with mapping capability from ~5 to 300 m. Both vessels have Applanix POS/MV motion sensors, which provide navigation and highly accurate readings of the vessel motion in all axes. Data were post-processed by the Pacific Islands Benthic Habitat Mapping Center (http://www.soest.hawaii.edu/pibhmc). IKONOS satellite imagery was used to create "estimated depths" and filled bathymetric gaps that existed within the 0–25 m depth range (Lyzenga 1985). Surface whitewash in the IKONOS image resulted in the identification of false depth estimates at select locations around Palmyra. These areas were manually removed and filled using a nearest neighbor interpolation method in ArcGIS Spatial Analyst (v 10.1, http://www.esri.com), resulting in a seamless 5 m bathymetry data set.

Waves: We incorporated a coupled hydrodynamic model developed by Delft Hydraulics (Delft3D; http://oss.deltares.nl/web/delft3d) to provide a high-resolution, nearshore spatial assessment of wave forcing at Palmyra. Each of the three models were run on a 7 x 20 km rectangular grid with a 50 m resolution and a 1 min time step over a 12 h period, with a coupling interval of 1 h between wave and current models. Water level (0.3 m) and winds (5 m s^{-1} from the northeast) were held constant over the model runs, representing average tidal and wind conditions for Palmyra. In the model, wave- and current-induced bed shear stress (BSS) were combined following parameterizations from (Soulsby et al. 1993) that account for the enhancement of BSS due to non-linear wave-current interactions. Following both numerical models and observations in similar coral reef environments, the wave friction factor was set to 0.3 (Péquignet et al. 2011, Van Dongeren et al. 2013), and the current friction factor was set to 0.2 (Hench et al. 2008, Lowe et al. 2009, Van Dongeren et al. 2013). The numerical model was run under all three wave regimes (i.e. northwest swell, northeast trade wind swell, and south swell) Palmyra is exposed to and combined to calculate an annual average maximum, mean, and range in H_s, t_p, and BSS.

Statistical analyses: To identify the spatial scale at which to investigate biophysical relationships without spatial autocorrelation, two techniques were employed: empirical semivariance (Meisel & Turner 1998) and lacunarity (Gefen et al. 1983, Mandelbrot 1983, Plotnick et al. 1993). Empirical semivariance, $\gamma(h)$ for separation h was calculated as follows:

$$\gamma(h) = \frac{1}{2N(h)} \sum_{i,j \in S(h)} (z_i - z_j)^2$$

where $N(h)$ is equal to the number of pairs of observations having separation h, $S(h)$ is the set of pairs of observations denoted by i and j that have separation h, and z_i is the benthic cover value for the i^{th} observation. The separations h were defined as:

$$h_{i,j} = j - i \; j - i \leq \frac{n}{2}$$
$$h_{i,j} = n - (j - i) \; j - i > \frac{n}{2}$$

where n is the number of discrete 50 m segments. Empirical semivariance calculations were completed using the *vgm* function in the *gstat* package (Pebesma 2004) linked to a custom coded function in R v2.15.1 (R Development Core Team, www.r-project.org). By plotting semivariance against distance, we were able to estimate at what point the relationship reached an asymptote, thus indicating the minimum distance required between sampling units to avoid spatial autocorrelation and achieve true independence of data points.

We further used lacunarity indices to avoid averaging over spatial distances that were either too large (i.e. averaging across true signal in the data) or too small (i.e. incorporating noise into the signal). Lacunarity assess how similar parts from different regions of a geometric object are to each other at a given scale (Gefen et al. 1983), thus providing an assessment of the scale of autocorrelation. Using a custom function in R, lacunarity was calculated as a function of window size, with the first and second derivatives plotted to aid interpretation. All points c within any window size s were taken to obtain a $_{mean}$ for that location. For a window situated at position i, this $_{mean}$ can be defined as:

$$\mu_i(s) = \frac{1}{\sum_{j=i}^{j=i+s-1} \delta_j} \sum_{j=i}^{j=i+s-1} c_j$$

where δ_j=1 if data are present and 0 otherwise. The window was then moved one unit further along and the next value obtained. For a given window size, we thus obtained a sequence of $_{mean}$ values $\mu_1(s)$, $\mu_2(s)$, $\mu_3(s)$……$\mu_n(s)$= $\boldsymbol{\mu}(s)$, where n is the number of sampling units. The lacunarity $l(s)$ for size s was defined as:

$$l(s) = 1 + \frac{var(\boldsymbol{\mu}(s))}{mean(\boldsymbol{\mu}(s)^2)}$$

Across all five benthic functional groups, both the empirical semivariance curves and the lacunarity indices indicated a non-independence of data at the 50 m segment scale. The semivariance curves showed a complete loss of spatial autocorrelation beyond distances of 500 m for all benthic categories, with the exception of macroalgae, and the lacunarity indices

indicated that 500 m was an optimal spatial scale at which to model the benthic data. We therefore scaled all the biological response variables and predictor variables (wave and geomorphological metrics) to a segment size of 500 m and only included segments ≥500 m apart during re-sampling of the data when creating independent data sets for our predictive modeling.

LITERATURE CITED

Gefen Y, Meir Y, Aharony A (1983) Geometric implementation of hypercubic lattices with noninteger dimensionality by use of low lacunarity fractal lattices. Phys Rev Lett 50: 145–148

Hench JL, Leichter JJ, Monismith SG (2008) Episodic circulation and exchange in a wave-driven coral reef and lagoon system. Limnol Oceanogr 53:2681–2694

Lowe R, Falter J, Monismith S, Atkinson M (2009) Wave-driven circulation of a coastal reef–lagoon system. J Phys Oceanogr 39:873–893

Lyzenga DR (1985) Shallow-water bathymetry using combined lidar and passive multispectral scanner data. Int J Remote Sens 6:115–125

Mandelbrot BB (1983) The fractal geometry of nature. WH Freeman, New York, NY

Meisel JE, Turner MG (1998) Scale detection in real and artificial landscapes using semivariance analysis. Landscape Ecol 13:347-362

Pebesma EJ (2004) Multivariable geostatistics in S: the gstat package. Comp Geosci 30:683–691

Péquignet AC, Becker JM, Merrifield MA, Boc SJ (2011) The dissipation of wind wave energy across a fringing reef at Ipan, Guam. Coral Reefs 30:71–82

Plotnick RE, Gardner RH, O'Neil RV (1993) Lacunarity indices as measures of landscape texture. Landscape Ecol 8:201–211

Soulsby RL, Hamm L, Klopman G, Myrhaug D, Simons RR, Thomas GP (1993) Wave-current interaction within and outside the bottom boundary layer. Coast Eng 21:41–69

Van Dongeren A, Lowe RJ, Pomeroy A, Trang DM, Roelvink D, Symonds G, Ranasinghe R (2013) Numerical modeling of low-frequency wave dynamics over a fringing coral reef. Coast Eng 73:178–190

Table S1. Summary of information pertaining to temperature drops by mooring location from April 2010 to May 2011. All data were sampled at 2.5 min intervals from ~20 m depth. Please see Fig. 2 and Table 1 in the main text for mooring locations and additional information pertaining to each mooring.

Total number of temperature drops: temperature change (°C)								
	0.3–0.5	**fraction**	**0.5–1.0**	**fraction**	**> 1.0**	**fraction**	**max**	Total
West	128	0.60	78	0.36	9	0.04	1.33	215
Northwest	67	0.66	31	0.30	4	0.04	1.48	102
Northeast	81	0.70	28	0.24	6	0.05	1.44	115
East	206	0.61	105	0.31	28	0.08	1.56	339
Southeast	77	0.58	40	0.30	15	0.11	1.73	132
Southwest	59	0.54	38	0.35	12	0.11	1.49	109
Total number of temperature drops: time elapsed to minimum temperature (min)								
	0–30	**fraction**	**30–120**	**fraction**	**120–720**	**fraction**	**max**	Total
West	36	0.17	94	0.44	85	0.40	542.5	215
Northwest	19	0.19	44	0.43	39	0.38	455	102
Northeast	23	0.20	52	0.45	40	0.35	422.5	115
East	60	0.18	176	0.52	103	0.30	560	339
Southeast	24	0.18	45	0.34	63	0.48	672.5	132
Southwest	15	0.14	57	0.52	37	0.34	522.5	109

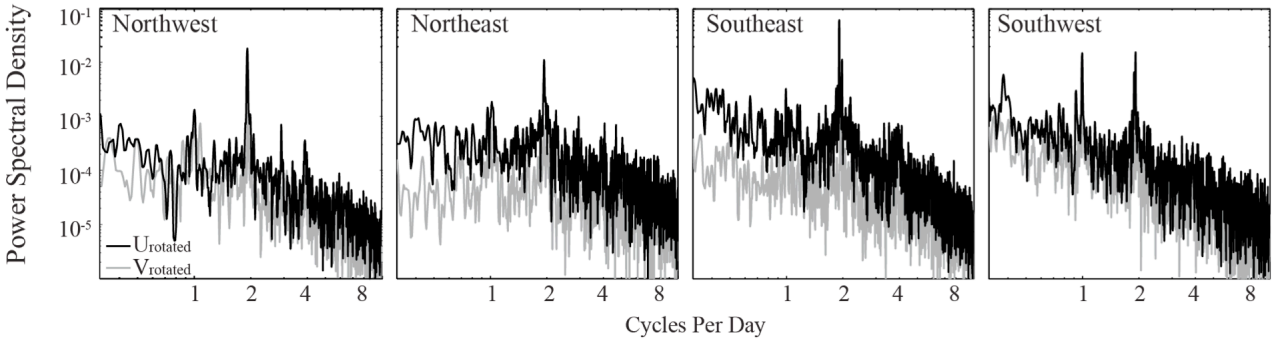

Fig S1. Power spectral density for horizontal currents (U and V components of current) rotated about their principle axis for the Northwest, Northeast, Southeast, and Southwest moorings, from right to left, respectively. Peaks are observed primarlily at diurnal (1 cycle per day or 23.924 h per cycle) and semi-diurnal (1.934 cycles per day or 12.421 h per cycle) tidal freqeuncies. Please see Fig. 2 in the main text for mooring locations.

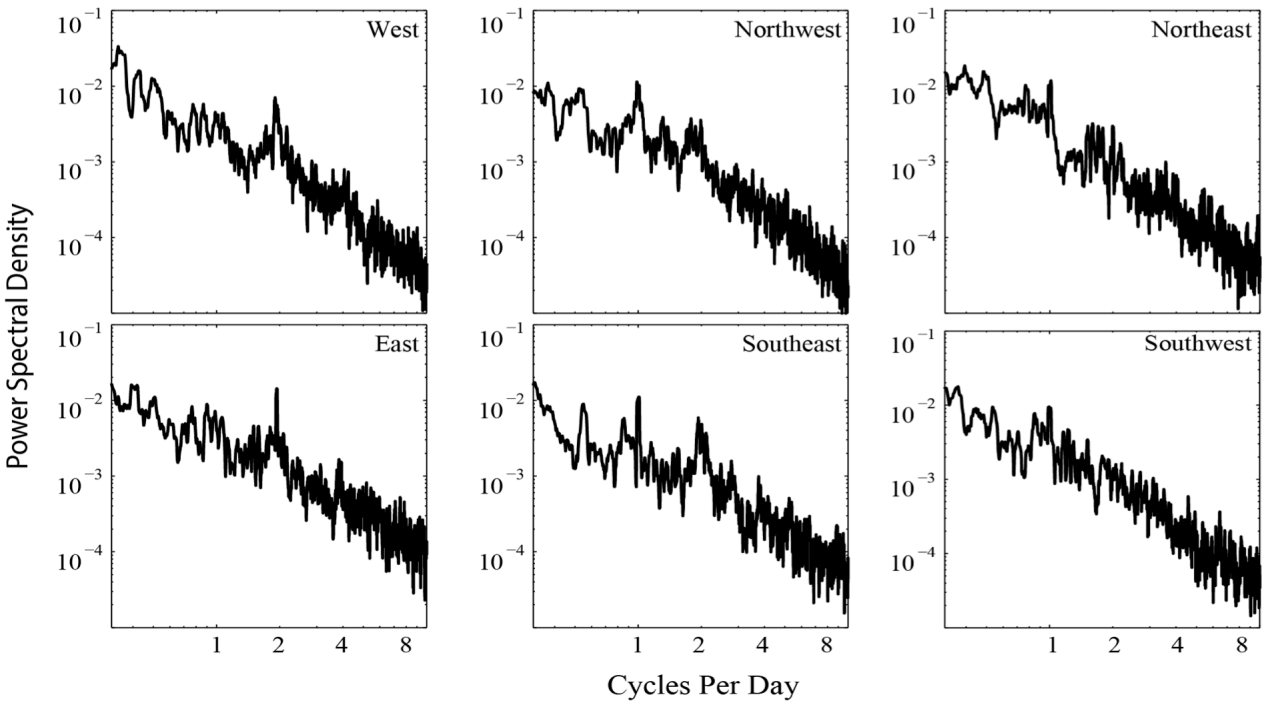

Fig S2. Power spectral density near-reef temperature collected from the West, Northwest, Northeast, Southeast, South and Southwest moorings. Spectral peaks indciate the dominant frequncies of temperature variability through time. Variability among locations predominantly at the diurnal (1 cycle per day or 23.924 h per cycle) or semi-diurnal (1.934 cycles per day or 12.421 h per cycle) tidal frequencies. Please see Fig. 2 in the main text for mooring locations.